CRYSTAL GROWTH & DESIGN

pubs.acs.org/crystal

Article

Nucleation of Aragonite ($CaCO_3$) from Monohydrocalcite ($CaCO_3.H_2O$) Slurries: Kinetics and Activation Energy from Raman Spectroscopy

German Montes-Hernandez* and Gabriel Montes

Cite This: https://doi.org/10.1021/acs.cgd.6c00259

Read Online

ACCESS | Metrics & More | Article Recommendations | Supporting Information

ABSTRACT: The ability to control the polymorph phase is one of the ultimate challenges in crystallization, where a key goal is to produce specific high-purity phases as required. Biomineralization processes are excellent examples, where organisms can select for specific polymorphs with perfect fidelity. In the present study, we report new insights into aragonite nucleation from monohydrocalcite slurry as a function of temperature (from room T (≈23 °C) to 90 °C) and as a function of initial ionic concentration at the same Mg/Ca molar ratio. Herein, competing monohydrocalcite and nesquehonite nucleation and aragonite nucleation from monohydrocalcite slurry were monitored in real time by using Raman spectroscopy. On the other hand, at higher concentrations, monohydrocalcite was purified from a monohydrocalcite and nesquehonite mixture by simple 2−3 successive washings using tap water. Here, nesquehonite is dissolved, leading to high-purity monohydrocalcite synthesis (more stable in tap water for this Ca−Mg system). As expected, the transformation kinetics from monohydrocalcite into aragonite is strongly dependent on the temperature and also on the residual Mg onto/into monohydrocalcite crystals. Herein, kinetic rate constants as a function of temperature were determined from the fitting of an empirical sigmoidal model. Then, kinetic rate constants were used to calculate the related activation energy by using the Arrhenius equation. This promising study then reports a simple method to synthesize massively high-purity monohydrocalcite, an emergent material to remove pollutants from water and as an additive in concrete materials (CO_2 sequestration and improving mechanical properties). In addition, we demonstrated that selected aragonite can be also produced abiotically at room temperature, systematically observed and attributed exclusively to the life of several sea shell animals.

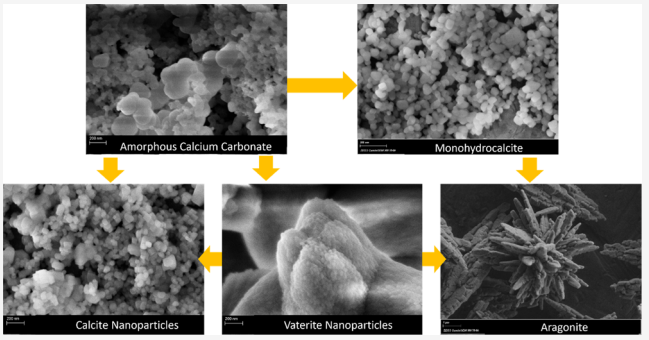

1. INTRODUCTION

In the nucleation and growth processes of crystals, polymorphism is a very common phenomenon in natural biotic or abiotic settings. It can also have a significant impact on the manufacturing processes and products (e.g., drugs).[1,2] In the lab or industry, different polymorphs can be generated by using different operating conditions, the use of different solvents, the presence or absence of impurities, application of different fluid hydrodynamic conditions, a heat-aging step (maturation temperature), or just with the passing of time (maturation time).[3,4] In fact, the ability to control polymorph phase is one of the ultimate challenges in crystallization, where a key goal is to produce specific high-purity phases upon requirement.[1−6] Some of the best examples of polymorph control are provided by the world of biomineralization, where organisms can select for specific polymorphs with perfect fidelity.[7−9] Concerning calcium carbonates, the synthesis of high-purity aragonite (metastable) or high-purity vaterite (unstable) via transformation of amorphous calcium carbonates or via transformation of crystalline transient phases (e.g., monohydrocalcite) remains a significant challenge.[10−12] Moreover, both aragonite and vaterite systems have been less investigated than calcite, the latter being the most stable calcium carbonate at standard pressure−temperature conditions.[13,14] In a biomineralization context, the aragonite polymorph is perfectly formed in several seashells and corals; however, its formation mechanism remains poorly understood and/or debated.[9,15] Its formation under abiotic lab conditions has been generally controlled by temperature (60−90 °C) and by the presence of Mg and/or organic molecules.[16,17] However, aragonite nucleation and/or synthesis at room temperature (T < 30 °C) under abiotic conditions remains an important challenge. In this way, the synthesis of monohydrocalcite precursor

Received: February 20, 2026
Revised: July 23, 2026
Accepted: July 24, 2026

($CaCO_3.H_2O$) and its transformation into aragonite has been investigated. During this mineral−mineral transformation, the sequestration of ionic pollutants has been claimed. In this manner, the removal of toxic anions from water has been investigated,[18] the impurity or pollutant sequestration favoring the monohydrocalcite-to-aragonite transformation at room T, but in general, calcite is preferentially formed. Monohydrocalcite-to-aragonite/calcite transformation has also been suggested to improve cement hydration in concrete manufacturing.[19] In this context, monohydrocalcite, which is a rare natural mineral currently identified in alkaline lakes, basaltic caves, and cold/humid mine galleries,[20] now appears as an emerging new material with high potential to remove toxic ions from water and with high potential to improve cement hydration properties.[18,19] However, monohydrocalcite has never been produced at an industrial scale to the best of our knowledge, and the synthesis methods proposed at the laboratory scale use low ionic concentrations.[11,21,22] In this way, the objective in the present study is 2-fold: first, a novel method using concentrated ionic solutions is proposed to synthesize monohydrocalcite massively, and second, its transformation into aragonite in tap water is also investigated from room T up to 90 °C. Herein, concurrent nucleation of monohydrocalcite and nesquehonite from amorphous calcium−magnesium carbonate slurry, monohydrocalcite purification/washing, and monohydrocalcite-to-aragonite transformation in tap water were monitored in real time by using Raman spectroscopy. This original spectroscopic method was recently used to determine nucleation processes of various carbonates, iron oxides, phosphate, and sulfate minerals.[23−30] In fact, the monitoring in real time using diversified analytical tools (X-ray scattering (SAXS/WAXS), X-ray absorption spectroscopy (EXAFS/XANES), atomic force and electron microscopies (AFM and TEM), Raman spectroscopy, etc.) and advanced numerical simulations has considerably contributed to the current knowledge on the mineral nucleation processes in the last decades.[31−34] At the present time, it is incrementally accepted that the formation of transient amorphous and/or crystalline phases occurs at the early stages during the crystallization process of a given metastable or stable crystal/mineral in aqueous systems. This crystallization pathway agrees with Ostwald's rule, but transient phases (preclusters, colloidal matter, gels, amorphous and crystalline phases) are not necessarily polymorphs; in fact, they can have different chemical compositions and different particle sizes. In this way, multistep nucleation events may exist and combine various reaction mechanisms at the solid−fluid interfaces. Thus, solid−state transition, dissolution−recrystallization, self-assembly aggregation, and partial dissolution−aggregation may operate together during nucleation and growth processes.[28,29,35−37] This recent crystallization conception in aqueous media and the use of time-resolved Raman spectroscopy measurements were then used to synthesize high-purity monohydrocalcite from amorphous calcium carbonate and then to investigate its transformation into aragonite in tap water as a function of temperature.

2. MATERIALS AND METHODS

2.1. Preparation of Divalent Cation Solutions

Concentrated Ca^{2+} (1 M) and Mg^{2+} (1 M) solutions were prepared by using $CaCl_2.2H_2O$ and $MgCl_2.6H_2O$ soluble salts, respectively. Herein, mixtures containing 40, 50, 60, and 75% of Mg were then prepared. Dilutions by 2, 5, and 10 factors containing 50% of Mg and Ca were also prepared.

2.2. Preparation of Alkaline Carbonate Solution

An alkaline carbonate solution was prepared in the lab by chemisorption of CO_2 in a soda solution. Here, a 2 M NaOH solution was used to capture the CO_2 as ionic species (CO_3^{2-} and HCO_3^-) at moderate pressure capture (P_{CO2} = 25 bar) and at room temperature. For this, 1 L of a NaOH solution (2 M) was placed in a reactor cell of 2 L of total capacity. Then, 25 bar of CO_2 was injected into the reactor. The pressure drop related to the CO_2 chemisorption process and exothermicity (temperature increase during CO_2 chemisorption) were directly monitored in this anisobaric system. In this particular system, CO_2 is completely chemisorbed in only several hours, leading to carbonate and bicarbonate ionic species, as monitored by Raman spectroscopy in selected experiments (see, e.g., Figure SI1).

2.3. Concurrent Nucleation of Monohydrocalcite and Nesquehonite

100 mL of Ca (1 M) and 100 mL of Mg (1 M) were first mixed, and then this binary ion solution was abruptly mixed with 200 mL of bicarbonate/carbonate solution, leading to a gel-like colloidal suspension instantaneously. This colloidal suspension was rapidly monitored with Raman spectroscopy for 24 h at room temperature (≈23 °C) with a spectral frequency of 1 min. Herein, the amorphous Ca−Mg phase was immediately detected, and its transformation into crystalline phases (Nesquehonite and monohydrocalcite) was directly monitored in real time by Raman spectroscopy, as already demonstrated for several mineral phases.[23−30] Nesquehonite and monohydrocalcite are transient mineral phases that can react with each other to form proto-dolomite (more stable phases) after various days, as claimed by Montes-Hernandez et al.[29] In the present study, a preferential synthesis of monohydrocalcite was envisaged. This means that nesquehonite needs to be removed from the slurry as described in the following subsection.

2.4. Monohydrocalcite Purification

Monohydrocalcite (MHC) was easily separated from nesquehonite (N) by simple repeated washing with tap water, 2−3 times, depending on the nesquehonite concentration in the slurry and on the amount of added water after each settling-water addition cycle step. Herein, nesquehonite is unstable in tap water, and it is rapidly dissolved, leading to high-purity monohydrocalcite as attested/monitored by Raman spectroscopy in the recovered suspensions/slurries. In practice, about 6 L of water is needed to purify 400 mL of synthesized MHC-N slurry. Obviously, this will be an important practical limitation at industrial scale, except if the produced Mg-rich water is reused in agriculture, for example. About the same amount of water is required using percolation systems (or dialysis purification method); however, the required time for purification is optimized from 12 h (batch system) to 2−3 h in flow-through systems. For the dialysis technique, some collected-time samples were characterized by using a portable multi-ion probe (from NT Sensors imacimus) in order to measure the ion concentration (Ca^{2+}, Mg^{2+}, Na^{-+}, NH_4^+, K^+, Cl^-, NO_3^-) and pH.

2.5. Monohydrocalcite Transformation into Aragonite

In order to measure the temperature effect with success on the monohydrocalcite-to-aragonite transformation, 600 mL of high-purity monohydrocalcite slurry was devised in 3 equal parts of 200 mL. This allows precise control of the solid−liquid ratio in the system. In this way, the effect of maturation temperature was then investigated at three different temperatures (RT (≈25), 60, and 90 °C). This simple strategy allows a realistic measurement of kinetic rates as a function of temperature, involving an overall monohydrocalcite-to-aragonite transformation. In practice, 200 mL of monohydrocalcite slurry was placed in a reactor with constant stirring (400 rpm), and the slurry was immediately monitored by Raman spectroscopy in real time in order to determine the kinetics and reaction mechanism during its transformation into aragonite. Similar to previous mineral nucleation

https://doi.org/10.1021/acs.cgd.6c00259
Cryst. Growth Des. XXXX, XXX, XXX−XXX

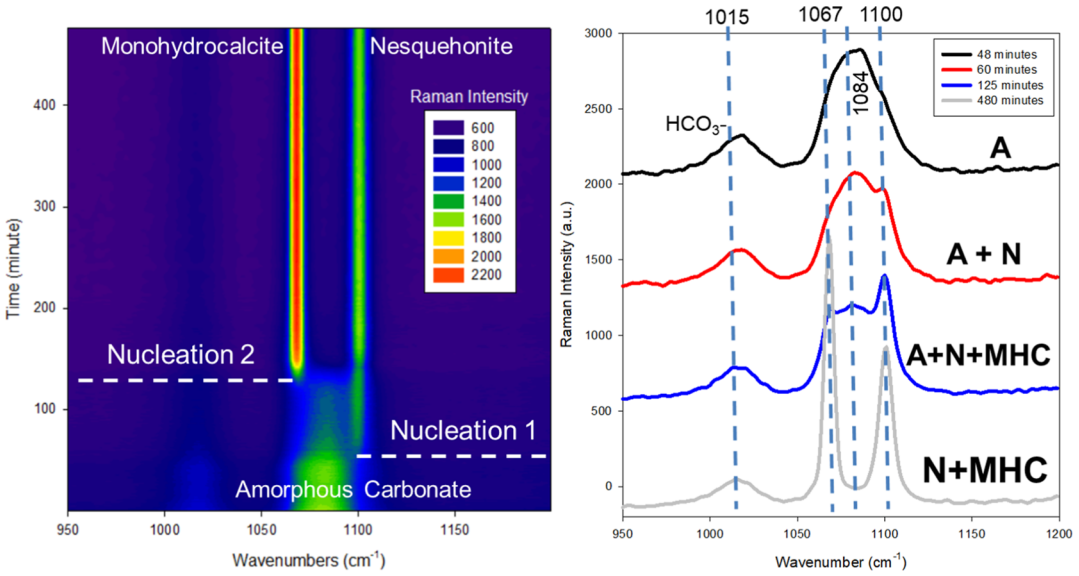

Figure 1. Concurrent nucleation of nesquehonite ($MgCO_3.3H_2O$) and monohydrocalcite ($CaCO_3.H_2O$) from amorphous calcium−magnesium carbonate (ACMC) slurry monitored in real time by Raman spectroscopy. A: amorphous calcium−magnesium carbonate (ACMC); N: nesquehonite; MHC: monohydrocalcite.

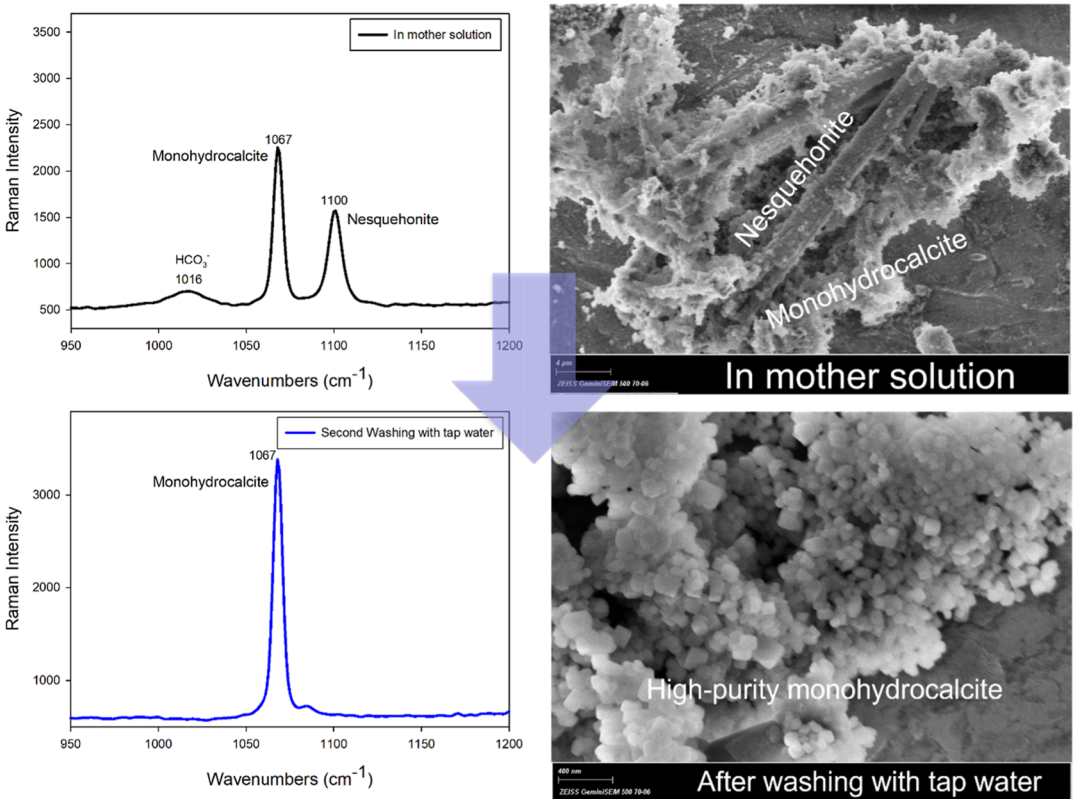

Figure 2. Monohydrocalcite purification from nesquehonite−monohydrocalcite slurry by simple washing with tap water. Here, nesquehonite dissolves in tap water and monohydrocalcite is stabilized with residual adsorbed magnesium as monitored ex situ by Raman spectroscopy and electron microscopy (FESEM).

experiments, the spectral time acquisition was imposed to 1 min during the first 3 h and then 5 min for 1 to 3 days. In fact, the experiments were stopped when monohydrocalcite was completely transformed into aragonite; i.e., the vibration mode at 1067 cm^{-1} for monohydrocalcite was no longer detected, and the vibration mode at 1086 cm^{-1} for aragonite reached spectral equilibration (constant Raman intensity).

2.6. Ex Situ Solid Characterization

The solid products were recovered by simple settling and, if necessary, washed twice with tap water in order to remove soluble salts. They were then dried in air at 60 °C for 24−48 h. The dried solid products were stored in plastic flasks for subsequent characterization of selected samples by field emission scanning electron microscopy (FESEM) and powder X-ray diffraction (XRD).

https://doi.org/10.1021/acs.cgd.6c00259
Cryst. Growth Des. XXXX, XXX, XXX−XXX

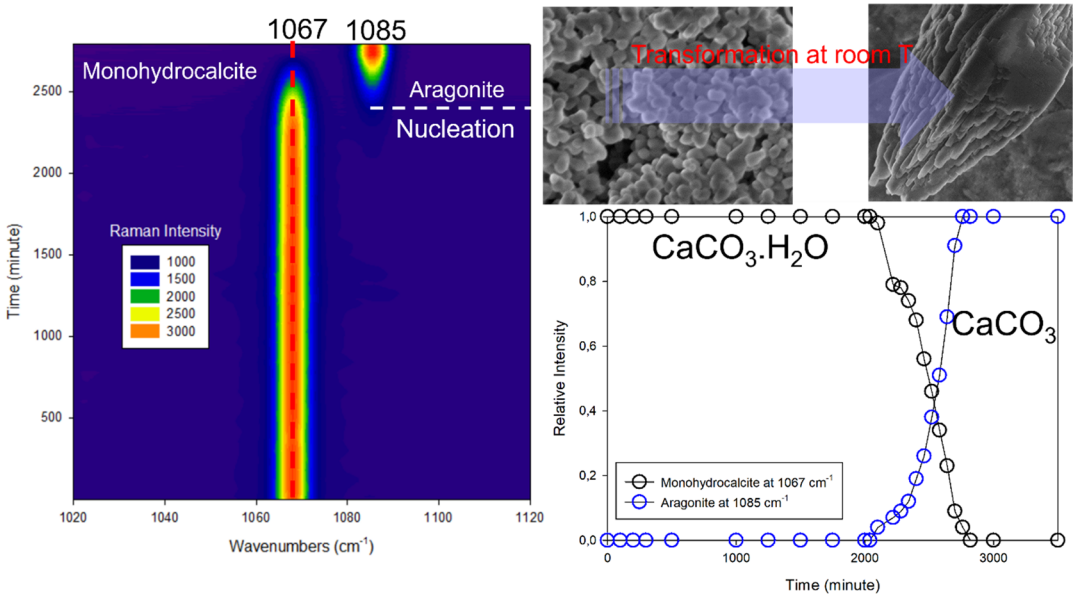

Figure 3. Aragonite nucleation from monohydrocalcite slurry at room temperature (≈25 °C) monitored in real time by Raman spectroscopy (vibration mode at 1085 cm^{-1}). FESEM images showing the crystal shape of monohydrocalcite (reactant) and aragonite (product). Transformation rate (relative Raman intensity vs time) is also illustrated using the strongest vibration modes for two phases; here, aragonite was differentiated from calcite or vaterite by using bending and lattice vibration modes.

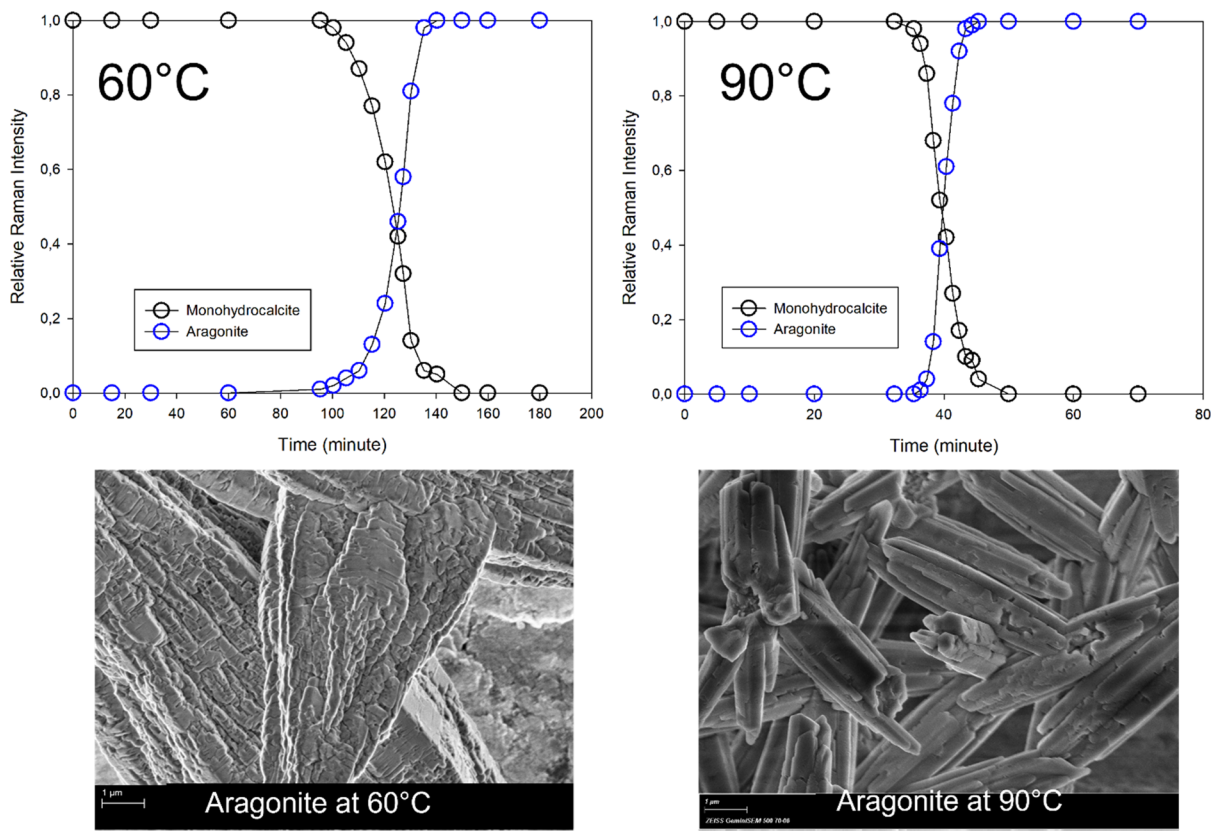

Figure 4. Aragonite nucleation from monohydrocalcite slurry at 60 and 90 °C monitored in real time by Raman spectroscopy (vibration mode at 1085 cm^{-1}). FESEM images showing the crystal shape of aragonite (product). The transformation rate (relative Raman intensity vs time) is also illustrated using the strongest vibration modes for two phases; here, aragonite was differentiated from calcite or vaterite by using bending and lattice vibration modes.

Powder XRD spectra were acquired using a Siemens D5000 diffractometer in Bragg−Brentano geometry, equipped with a theta−theta goniometer with a rotating sample holder. Diffraction patterns were collected using Cu kα_1 ($\lambda_{k\alpha1}$ = 1.5406 Å) and Cu kα_2 ($\lambda_{k\alpha2}$ = 1.5444 Å) radiation in the range of 2θ = 10−70°, with a step size of 0.04° and a counting time of six seconds per step. For high-resolution imaging, the solid products were dispersed by ultrasonic treatment in absolute ethanol for 5 min. Two droplets of the suspension were then

https://doi.org/10.1021/acs.cgd.6c00259
Cryst. Growth Des. XXXX, XXX, XXX−XXX

deposited directly onto an aluminum support and observed without metal coating to avoid any surface perturbation at high magnification. The powders were imaged using a Zeiss Ultra 55 FESEM with a maximum spatial resolution of approximately 1 nm at 15 kV.

2.7. Fitting of Kinetic Data

Monohydrocalcite transformation into aragonite is characterized by two well-separated peaks at 1067 and 1086 cm^{-1}, respectively; except when calcite is also formed in the system, in such cases, the calcite and aragonite stretching vibration modes are overlapped. In our study, aragonite was only formed, and it was spectrally controlled with the detection of bending and lattice vibration modes that are specific/discriminate for each carbonate phase (see Figure SI2). In this well-controlled case (oriented crystallization), the aragonite nucleation from monohydrocalcite slurry and the kinetic transformation were then monitored in real time until a given spectral equilibration with time, i.e., until monohydrocalcite is no longer detected and the aragonite Raman peak intensity is constant with time (spectral equilibration). In this way, the relative intensity behavior with time for aragonite (λ vs t) was simplified by using a conventional sigmoidal model as follows

$$\lambda = \frac{1}{1 + \exp(-((t - t_{max})/b))} \quad (1)$$

where t_{max} is the inflection point, i.e., the time at which 50% of aragonite formation was reached (λ = 0.5). In this way, the kinetic rate constant is ($1/t_{max}$); b is also a kinetic parameter related to the sigmoidal model.

2.8. Calculation of Activation Energy

Typically, the kinetic rate constant ($1/t_{max}$) as a function of temperature (T) can be fitted by the Arrhenius equation in order to determine the activation energy (E_a) as follows

$$\frac{1}{t_{max}} = A e^{-E_a/RT} \quad (2)$$

The linearized form of the Arrhenius equation facilitates the estimation of activation energy as follows

$$\ln \frac{1}{t_{max}} = \ln A - \frac{E_a}{RT} \quad (3)$$

This simple mathematical linear arrangement reduces the required experiments for a successful calculation of activation energy. Herein, three temperatures were mainly investigated (room $T \approx 25$, 60, and 90 °C) using the same solid/liquid ratio. The experiments were triplicated.

3. RESULTS AND DISCUSSION

3.1. Concurrent Nucleation of Monohydrocalcite and Nesquehonite

As already demonstrated, the abrupt mixture of Ca−Mg and carbonate-alkaline solutions leads to an instantaneous formation of an amorphous calcium−magnesium carbonate (ACMC) phase. Herein, when the Mg/Ca molar ratio is >0.4 and the ionic concentration is >0.1 M, the amorphous carbonate phase is systematically transformed into nesquehonite (first-step nucleation from ACMC slurry), followed by monohydrocalcite (second-step nucleation), as monitored in real time by Raman spectroscopy (Figure 1). Here, the precipitated ACMC is characterized by a broad Raman peak at 1084 cm^{-1}; time-resolved Raman spectroscopy in Figure 1 shows that ACMC starts transforming into crystalline phases after about 60 min of reaction. Nesquehonite ($MgCO_3.3H_2O$) is the first detected phase, with a peak at 1100 cm^{-1} and a nucleation time of 60 min (±10 min), followed by monohydrocalcite ($CaCO_3.H_2O$), with a peak at 1067 cm^{-1} and a nucleation time of 125 min (±19 min) (Figure 1 and see also Figure SI3). Both crystallization reactions from the amorphous phase were already suggested in our previous study on the proto-dolomite formation.[29] In fact, nesquehonite and monohydrocalcite are transient phases that may be progressively transformed into proto-dolomite, a more stable phase, if ideal conditions exist.[29] In the present study, the nucleation time for nesquehonite and monohydrocalcite corresponds to the first detectable Raman spectroscopy signal as indicated in the Raman map using dotted horizontal lines (in white) in Figure 1 (plot on the left). We also note that the nucleation time for nesquehonite and monohydrocalcite and/or the lifetime of the amorphous phase are strongly dependent on the initial ionic concentration; in fact, the lifetime increases with a decrease of ionic concentration. Moreover, for diluted ionic concentrations (C ≤ 0.05 M), nesquehonite formation is inhibited at room temperature. In this case, monohydrocalcite is only detected by Raman spectroscopy (see Figure SI4). This is an interesting result from the perspective of synthesizing and/or stabilizing high-purity monohydrocalcite; however, the produced amount of monohydrocalcite is slight in batch systems at these concentrations. Obviously, higher amounts of

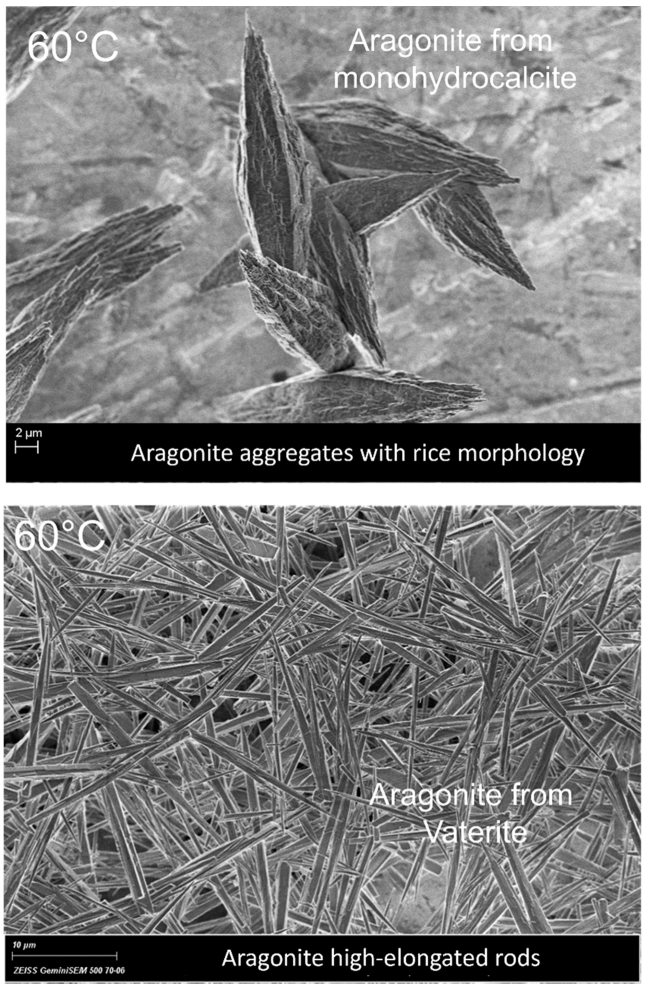

Figure 5. High-purity aragonite with different sizes and shapes of crystals by using two different precursors or transient phases. Top FESEM image illustrating aragonite aggregates with rice morphology obtained by monohydrocalcite-to-aragonite transformation at 60 °C. Bottom FESEM image illustrating aragonite-elongated rods obtained by vaterite-to-aragonite transformation directed by Mg ions at 60 °C.

https://doi.org/10.1021/acs.cgd.6c00259
Cryst. Growth Des. XXXX, XXX, XXX−XXX

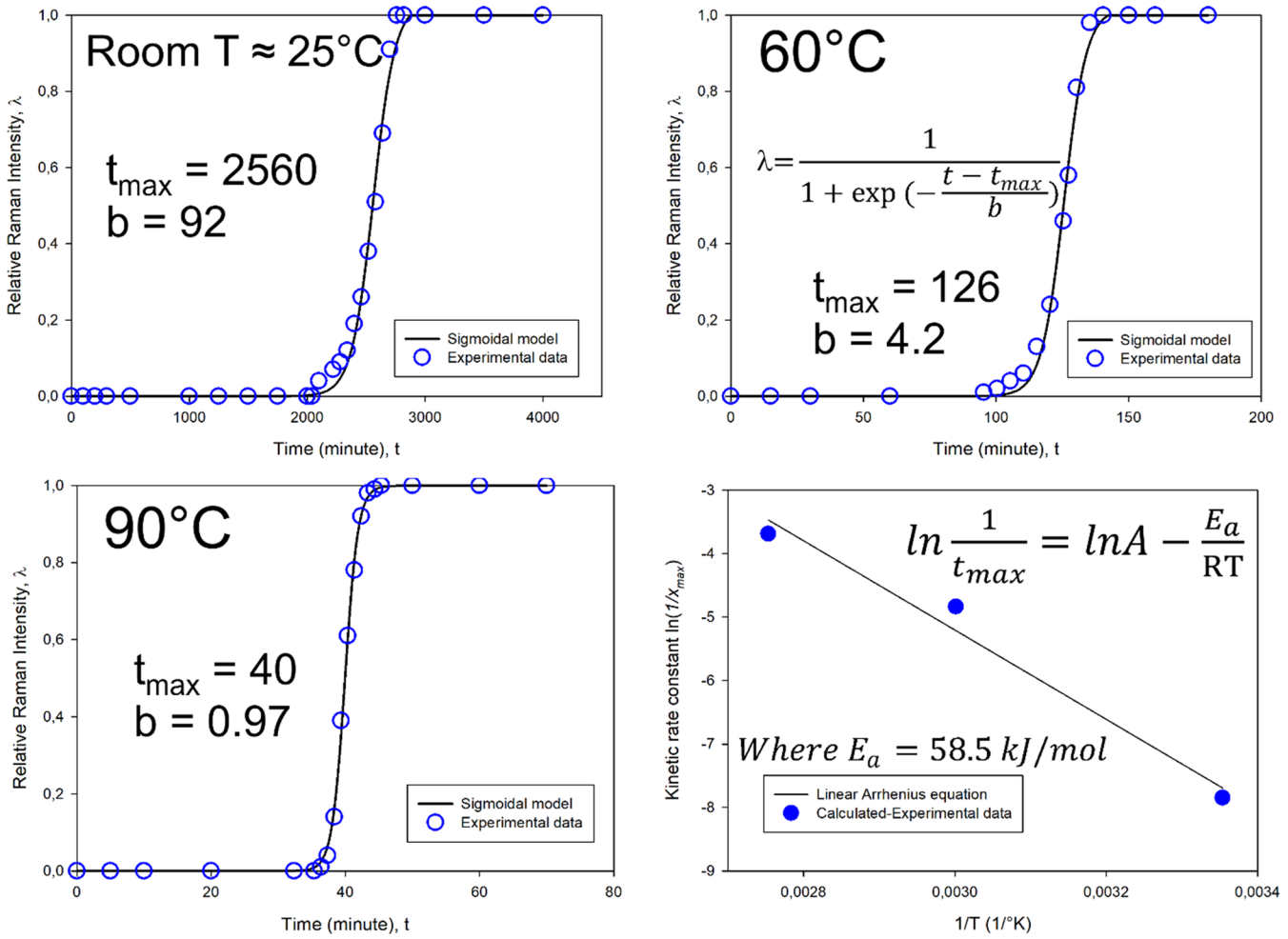

Figure 6. Fitting of kinetic behavior for aragonite formation from monohydrocalcite slurry by using a simple sigmodal model (two kinetic parameters). Determination of activation energy by using the linearized Arrhenius equation.

monohydrocalcite can be produced using higher ionic concentrations of solutions, but a given purification of monohydrocalcite is required because nesquehonite is also precipitated as described in the following subsection.

3.2. Purification of Monohydrocalcite from the Monohydrocalcite-Nesquehonite Mixture

In recent years, monohydrocalcite has been suggested as an emergent mineral to recycle/store carbon dioxide (CCUS) and also to remove toxic ions from water.[18,19] However, this mineral has never been produced at industrial scale, and in the literature, the use of low ionic concentrations to produce monohydrocalcite is only reported.[11,21,22] In the present study, the use of concentrated ionic solutions allows a rapid production of monohydrocalcite ($CaCO_3.H_2O$) at room temperature (≈25 °C) in only a few hours. However, the nesquehonite ($MgCO_3.3H_2O$) is also formed in the system as explained above and summarized in Figure 1. This hydrated magnesium carbonate phase is very unstable in tap water. Based on this assumption, two possibilities are considered here: first, if a high-purity monohydrocalcite is targeted, a simple purification by washing with tap water can be used. In this way, the nesquehonite is preferentially dissolved, and then high-purity monohydrocalcite can be obtained as illustrated in Figure 2 and also verified in powdered samples by infrared spectroscopy and X-ray diffraction (see Figure SI5). Here, submicrometric crystals of monohydrocalcite can be stabilized for weeks and/or months as suspensions or as a powdered material, but a residual amount of fixed magnesium onto monohydrocalcite seems crucial because if all magnesium is removed by washing or when pH is close to tap water (e.g., dialysis/percolating experiments), monohydrocalcite is rapidly transformed into calcite and, in this case, aragonite and calcite coexist in suspension and as powder (see, e.g., Figure SI6). Here, the ion concentration in collected-time samples shows clearly that Mg from nesquehonite dissolution is rapidly released into the output solution, and monohydrocalcite remains in equilibrium with the interacting solution during the tap water percolation in the system (see Figure SI7). Following this simple washing method, monohydrocalcite was successfully stabilized in the interacting solution, and its transformation into aragonite was then perfectly controlled as a function of temperature. Then, the energetic requirements (e.g., activation energy) were easily determined as described in the following subsection. In practice, the purification of monohydrocalcite requires a high amount of tap water in order to remove the nesquehonite phase, and dissolved magnesium cannot be easily recovered. The use of polluted water with toxic ions from industrial processes, for example, could be a sustainable possibility, i.e., the removal of toxic ions onto monohydrocalcite as already suggested.[18] A second possibility is the recovery of the monohydrocalcite−nesque-

https://doi.org/10.1021/acs.cgd.6c00259
Cryst. Growth Des. XXXX, XXX, XXX−XXX

honite mixture as a powdered material. Obviously, this carbonate mixture material can find several uses as an additive in construction materials, plastics, paper, etc. We note, for example, that both minerals were already proposed as additives in cement material in order to improve its hydration properties with simultaneous carbon dioxide storage.[19,38] However, their thermodynamic instability under Earth's surface conditions could impact the concrete textural and mechanical properties in the long term. For this reason, anhydrous carbonate materials (magnesite ($MgCO_3$), dolomite ($MgCa(CO_3)_2$, calcite ($CaCO_{3(\text{trigonal system})}$), aragonite ($CaCO_{3(\text{orthorhombic})}$), etc.) are preferentially suggested as a partial substitute for cement in concrete manufacturing, with the perspective of storing industrial carbon dioxide without a significant negative impact on the concrete textural properties.[24]

3.3. Aragonite Nucleation from Monohydrocalcite Slurry at Room Temperature (≈25 °C)

In the crystallization of minerals or drugs, the ultimate challenge is the ability to control high-purity and polymorph phases. Concerning anhydrous calcium carbonates, three polymorphs exist (calcite, aragonite, and vaterite), and their selective formation in aqueous media under abiotic conditions is still strongly debated, as commented in the Introduction.[12,13] As already commented in the literature, the magnesium chemistry and organic additives play a determinant role in the formation of calcium carbonate polymorphs. At room temperature, calcite is easily formed, but Mg or organic additives are frequently used to control the size, shape, and organization of calcite crystals (e.g., synthesis of calcite mesocrystals[39]). Vaterite synthesis has been less investigated, but several methods have been proposed to produce high-purity vaterite at room temperature, as recently reported by our team.[40] Herein, Mg and/or organic additives have frequently been used to stabilize vaterite as a powder material or in suspension. Mg can also direct its transformation into aragonite instead of calcite, as claimed by Pimentel et al.[40] Concerning the aragonite polymorph, its abiotic synthesis at room temperature has not been claimed to the best of our knowledge. Here, we demonstrated that monohydrocalcite (a transient hydrated phase, $CaCO_3.H_2O$) in the presence of Mg ions can be transformed into aragonite at room temperature via a dissolution−recrystallization pathway as summarized in Figure 3. In fact, the Raman spectroscopy measurements in real time have revealed a proportional intensity decrease of the monohydrocalcite peak at 1067 cm^{-1} coupled with a proportional intensity increase of the aragonite peak at 1085 cm^{-1} until spectral equilibration (Figure 3). The bending peak at 704 cm^{-1} and lattice peak at 205 cm^{-1} (see Figure SI2) were also used to control the aragonite purity because, in some cases, calcite can also be formed in the system. In summary, three possibilities exist at room temperature in our investigated system:[1] oriented transformation of monohydrocalcite into high-purity aragonite, a slow kinetic transformation process as illustrated in Figure 3,[2] concurrent aragonite and calcite formation from monohydrocalcite slurry when Mg in not enough in the system, clearly detected by Raman spectroscopy when washing is excessive or pH is close to tap water, and[3] long-time monohydrocalcite stabilization in suspension when Mg is in excess as attested by a slight signal for nesquehonite phase at 1100 cm^{-1}. In this latter case, monohydrocalcite can remain stabilized as a powder material or in suspension for months. All of these insights allow a simple abiotic control using Mg as an additive in order to synthesize selected aragonite polymorphs, an ultimate challenge in crystallization. As expected, size, shape, agglomeration, and transformation kinetics of aragonite crystals can also be controlled by maturation temperature of monohydrocalcite slurries as discussed in the following section.

3.4. Aragonite Nucleation from Monohydrocalcite Slurry at 60 and 90 °C

As commented in the Introduction, the aragonite synthesis in the laboratory has been systematically performed under mild conditions (70−90 °C) using mainly Mg and organic compounds as additives.[16,17] This has led to confusing interpretations in the literature, sometimes claiming that aragonite is only formed under biotic conditions at room temperature (e.g., sea shells).[3−9] As discussed in the above subsection, aragonite can also be formed at room temperature under abiotic conditions via the transformation of monohydrocalcite into aragonite (Figure 3). This same transformation reaction was also investigated at 60 and 90 °C, and the results are summarized in Figure 4. Herein, significant effects were observed:[1] at 60 °C, aragonite crystallites were regularly oriented, leading to a rice morphology of micrometric aggregates (FESEM images in Figure 4). Conversely, at 90 °C, the stacked rods led to acicular aragonite microcrystals (FESEM images in Figure 4).[2] The aragonite nucleation time from monohydrocalcite slurry is strongly reduced with temperature, passing from some days at room temperature to only some minutes at 90 °C, as clearly illustrated by time-resolved Raman spectroscopy measurements in Figures 3 and 4. In summary, the monohydrocalcite transformation into aragonite remains a well-controlled option to synthesize high-purity aragonite as a function of temperature. Moreover, crystalline textural properties (size, shape, and organization) and transformation kinetics can be easily controlled under simple abiotic mild conditions. Kinetic measurements by Raman spectroscopy as a function of temperature then allow the estimation of activation energy for aragonite nucleation from monohydrocalcite slurry as described in the following subsection.

3.5. Monohydrocalcite-to-Aragonite Transformation Kinetics and Activation Energy

In crystallization processes, polymorphism is frequent for minerals and drugs; for example, for anhydrous calcium carbonates, three polymorphs exist: vaterite (unstable), aragonite (metastable), and calcite (stable). Despite the fact that several methods have been reported to synthesize calcium carbonate, the synthesis of high-purity vaterite and aragonite remains challenging. Our research team has recently published a study to synthesize high-purity vaterite.[23,40] The vaterite polymorph is unstable and in general is rapidly transformed into calcite in solution and under humid conditions. However, vaterite can also be stabilized for long durations with magnesium ions onto the vaterite nanocrystals, forming rounded porous aggregates with high specific surface area.[40] The sequestered magnesium onto vaterite crystals can also direct its transformation into aragonite instead of calcite; however, a long time is required at room temperature (weeks and/or months) or only some days at higher temperature (<90 °C). Preliminary results have revealed the aragonite synthesis from vaterite slurry at 60 °C. Herein, aragonite crystals are characterized by high-elongated rods as depicted by FESEM images (see Figure 5). Concerning the aragonite nucleation

https://doi.org/10.1021/acs.cgd.6c00259
Cryst. Growth Des. XXXX, XXX, XXX−XXX

from monohydrocalcite slurry, the nucleation time for aragonite decreases significantly with maturation temperature, as summarized in Figure 6. Herein, time-resolved Raman spectroscopy measurements have revealed a sigmoidal behavior for the three investigated temperatures. This kinetic behavior was then fitted by eq 1, and the obtained fitting parameters were directly indicated in Figure 6 for each temperature. In this way, the linearized form of the Arrhenius equation (eq 3) was then used to estimate the activation energy (E_a = 58.5 kJ/mol ±3 kJ/mol). This apparent activation energy concerns only the transformation of monohydrocalcite into aragonite, underlining that monohydrocalcite formation from a mixture of ionic solutions also implies the formation of a transient amorphous phase as described above. In fact, the nonclassical crystallization pathway for calcium carbonates was clearly characterized by Raman spectroscopy in real time.

In summary, the monohydrocalcite-to-aragonite transformation concerns various complex interfacial reactions, including dissolution of monohydrocalcite and nucleation and growth processes of aragonite, both processes probably also combined with oriented aggregation (see, e.g., Figure SI8). In a general picture, the Johnson−Mehl−Avrami−Kolmogorov (JMAK) empirical equation (also called the Avrami equation) has often been used to describe the progress of phase transformations in material systems. However, this method was originally developed on the classical nucleation theory (CNT), where the two fitting parameters of the Avrami equation are only based on speculative assumptions. In our opinion, it is difficult to relate the Raman spectroscopy signal to the combined textural properties of reacting particles during monohydrocalcite-to-aragonite transformation. For this reason, the sigmoidal kinetic equation was only used to determine the kinetic rate constants as a function of temperature.

4. CONCLUSION

The capability to control vaterite, aragonite, or calcite polymorph phase is one of the ultimate challenges in crystallization in the laboratory or at the industrial scale, where a key goal is to produce specific high-purity phases to meet the requirement. In this perspective and based on the nonclassical nucleation picture, we claim some relevant points in the present study.

1. The original method to synthesize high-purity and stabilized monohydrocalcite ($CaCO_3.H_2O$) using concentrated ionic solutions is a rare mineral in nature but an emergent mineral to store carbon dioxide and remove toxic ions from water. Its nucleation from an amorphous carbonate phase was monitored by Raman spectroscopy in real time.
2. The aragonite nucleation from monohydrocalcite in the presence of Mg ions is a kinetically slow process but controllable and measurable at room temperature by Raman spectroscopy in real time.
3. The kinetic transformation of monohydrocalcite into aragonite is significantly accelerated with temperature, as directly measured by Raman spectroscopy and experimental data fitted successfully with a conventional sigmoidal equation.
4. The linearized form of the Arrhenius equation was finally used to estimate the apparent activation energy (E_a = 58.5 kJ/mol) concerning the heterogeneous transformation of monohydrocalcite into aragonite.

■ ASSOCIATED CONTENT

Data Availability Statement

The data that support the findings of this study are available from the corresponding authors upon reasonable request.

Supporting Information

The Supporting Information is available free of charge at https://pubs.acs.org/doi/10.1021/acs.cgd.6c00259.

Complementary Raman spectroscopy measurements, microscopic observations (FESEM images), X-ray diffraction for selected samples, and ion concentration for some time-collected samples (PDF)

■ AUTHOR INFORMATION

Corresponding Author

German Montes-Hernandez − *CNRS, IRD, Univ. Gustave Eiffel, ISTerre, Univ. Grenoble Alpes, Grenoble INP, Univ. Savoie Mont Blanc, Grenoble 38000, France*; orcid.org/0000-0002-6692-3903; Email: german.montes-hernandez@univ-grenoble-alpes.fr

Author

Gabriel Montes − *CNRS, IRD, Univ. Gustave Eiffel, ISTerre, Univ. Grenoble Alpes, Grenoble INP, Univ. Savoie Mont Blanc, Grenoble 38000, France*

Complete contact information is available at: https://pubs.acs.org/10.1021/acs.cgd.6c00259

Notes

The authors declare no competing financial interest.

■ ACKNOWLEDGMENTS

The authors acknowledge funding from the French National Centre for Scientific Research (exploratory project PEPS-CNRS 2023 and multidisciplinary project MITI-CNRS 2024-2025).

■ REFERENCES

(1) Cardew, P. T. Ostwald Rule of Stages - Myth or Reality? *Cryst. Growth Des.* **2023**, *23*, 3958−3969.

(2) Khanjani, M.; Westenberg, D. J.; Kumar, A.; Ma, H. Tuning Polymorphs and Morphology of Microbially Induced Calcium Carbonate: Controlling Factors and Underlying Mechanisms. *ACS Omega* **2021**, *6*, 11988−12003.

(3) Amos, F. F.; Sharbaugh, D. M.; Talham, D. R.; Gower, L. B.; Fricke, M.; Volkmer, D. Formation of Single-Crystalline Aragonite Tablets/Films via an Amorphous Precursor. *Langmuir* **2007**, *23*, 1988−1994.

(4) Huang, Z.; Zhang, G. Biomimetic Synthesis of Aragonite Nanorod Aggregates with Unusual Morphologies Using a Novel Template of Natural Fibrous Proteins at Ambient Condition. *Cryst. Growth Des.* **2012**, *12*, 1816−1822.

(5) Nassif, N.; Gehrke, N.; Pinna, N.; Shirshova, N.; Tauer, K.; Antonietti, M.; Cölfen, H. Synthesis of Stable Aragonite Superstructures by a Biomimetic Crystallization Pathway. *Angew. Chem., Int. Ed.* **2005**, *44*, 6004−6009.

(6) Molnár, Z.; Pekker, P.; Rečnik, A.; Pósfai, M. Formation and Properties of Spindle-Shaped Aragonite Mesocrystals from Mg-bearing Solutions. *Nanoscale* **2024**, *16*, 2012−2021.

(7) Du, L.; Wang, Y.; Wang, K.; Luo, G. Growth of Aragonite CaCO3 Whiskers in a Microreactor with Calcium Dodecyl Benzenesulfonate as a Control Agent. *Ind. Eng. Chem. Res.* **2015**, *54*, 7131−7140.

(8) Boon, M.; Rickard, W. D. A.; Rohl, A. L.; Jones, F. Stabilization of Aragonite: Role of Mg^{2+} and Other Impurity Ions. *Cryst. Growth Des.* **2020**, *20*, 5006−5017.
(9) Chen, S. A.; Weber, J.; Starchenko, V.; Eng, P. J.; Stubbs, J. E.; Wang, H.-W.; Liu, T.; Spano, T. L.; Chakoumakos, B. C.; Stack, A. G. Real-Time Atomic-Scale Structural Analysis Resolves the Amorphous to Crystalline CaCO3Mechanism Controversy. *Cryst. Growth Des.* **2024**, *24*, 5027−5038.
(10) Williams, J. M.; Zhao, D.; Zhang, N.; Chin, A.; Kawashima, S.; Moment, A. J. Directed Synthesis of Aragonite through Semi-continuous Seeded Crystallization Methods for CO_2 Utilization. *CrystEngComm* **2023**, *25*, 6050−6066.
(11) Liu, R.; Liu, F.; Zhao, S.; Su, Y.; Wang, D.; Shen, Q. Crystallization and Oriented Attachment of Monohydrocalcite and its Crystalline Phase Transformation. *CrystEngComm* **2013**, *15*, 509−515.
(12) Santos, R. M.; Ceulemans, P.; Van Gerven, T. Synthesis of Pure Aragonite by Sonochemical Mineral Carbonation. *Chem. Eng. Res. Des.* **2012**, *90*, 715−725.
(13) Siva, T.; Muralidharan, S.; Sathiyanarayanan, S.; Manikandan, E.; Jayachandran, M. Enhanced Polymer Induced Precipitation of Polymorphous in Calcium Carbonate: Calcite Aragonite Vaterite Phases. *J. Inorg. Organomet. Polym. Mater.* **2017**, *27*, 770−778.
(14) Eichinger, S.; Boch, R.; Baldermann, A.; Goetschl, K.; Wenighofer, R.; Hoffmann, R.; Stamm, F.; Hippler, D.; Grengg, C.; Immenhauser, A.; Dietzel, M. Unravelling Calcite-to-Aragonite Evolution from a Subsurface Fluid -Formation Pathway, Interfacial Reactions and Nucleation Effects. *Chem. Geol.* **2023**, *641*, 121768.
(15) Greer, H. F.; Zhou, W.; Guo, L.; Guo, L. Phase Transformation of Mg-calcite to Aragonite in Active-Forming Hot Spring Travertines. *Miner. Petrol.* **2015**, *109*, 453−462.
(16) Fermani, S.; Njegić Džakula, B.; Reggi, M.; Falini, G.; Kralj, D. Effects of Magnesium and Temperature Control on Aragonite Crystal Aggregation and Morphology. *CrystEngComm* **2017**, *19*, 2451−2455.
(17) Aquilano, D.; Bruno, M.; Pastero, L. Impurity Effects on Habit Change and Polymorphic Transitions in the System: Aragonite−Calcite−Vaterite. *Cryst. Growth Des.* **2020**, *20*, 2497−2507.
(18) Fukushi, K.; Munemoto, T.; Sakai, M.; Yagi, S. Monohydrocalcite: a Promising Remediation Material for Hazardous Anions. *Sci. Technol. Adv. Mater.* **2011**, *12*, 064702.
(19) Photong, C.; Pragot, W. Effect of Adding Monohydrocalcite on the Microstructural Change in Cement Hydration. *ACS Omega* **2022**, *7*, 36318−36329.
(20) Rodriguez-Blanco, J. D.; Shaw, S.; Bots, P.; Roncal-Herrero, T.; Benning, L. G. The Role of Mg in the Crystallization of Monohydrocalcite. *Geochim. Cosmochim. Acta* **2014**, *127*, 204−220.
(21) Nishiyama, R.; Munemoto, T.; Fukushi, K. Formation Condition of Monohydrocalcite from $CaCl_2$-$MgCl_2$-Na_2CO_3 Solutions. *Geochim. Cosmochim. Acta* **2013**, *100*, 217−231.
(22) Fukushi, K.; Suzuki, Y.; Kawano, J.; Ohno, T.; Ogawa, M.; Yaji, T.; Takahashi, Y. Speciation of Magnesium in Monohydrocalcite: XANES, ab Initio and Geochemical modeling. *Geochim. Cosmochim. Acta* **2017**, *213*, 457−474.
(23) Montes-Hernandez, G. Decarbonizing the Cement Industry is Crucial for Reducing CO2 Emissions: Myth or Reality? *Chem. Eng. J.* **2025**, *518*, 164995.
(24) Montes-Hernandez, G.; Weiss, J.; Clavier, S.; Cordonnier, B.; Tafforeau, P.; Plé, O.; Renard, F. Fabrication of Iron-magnesite under Mild Conditions through Indirect Carbonation of Peridotite and its Utilization as Partial Substitute for Cement in Concrete. *Ind. Eng. Chem. Res.* **2025**, *64*, 13770−13783.
(25) Stawski, T. M.; Karafiludis, S.; Pimentel, C.; Montes-Hernandez, G.; Kochovski, Z.; Bienert, R.; Weimann, K.; Emmerling, F.; Scoppola, E.; Van Driessche, A. E. S. Solution-driven Processing of Calcium Sulfate: the Mechanism of the Reversible Transformation of Gypsum to Bassanite in Brines. *J. Clean. Prod.* **2024**, *440*, 141012.
(26) Montes-Hernandez, G. Magnesite Formation from Nesquehonite Slurry at 90°C using some Soluble Mg Salts: Eitelite as an Atypical Transient Mineral Phase. *Chem. Eng. Sci.* **2024**, *287*, 119776.
(27) Montes-Hernandez, G.; Findling, N.; Renard, F. Direct and Indirect Nucleation of Magnetite Nanoparticles from Solution Revealed by Time-Resolved Raman Spectroscopy. *Cryst. Growth Des.* **2021**, *21*, 3500−3510.
(28) Montes-Hernandez, G.; Renard, F. Nucleation of Brushite and Hydroxyapatite from Amorphous Calcium Phosphate Phases Revealed by Dynamic in situ Raman Spectroscopy. *J. Phys. Chem. C* **2020**, *124*, 15302−15311.
(29) Montes-Hernandez, G.; Renard, F.; Auzende, A.-L.; Findling, N. Amorphous Calcium-Magnesium Carbonate (ACMC) accelerates Dolomitization at Room Temperature under Abiotic Conditions. *Cryst. Growth Des.* **2020**, *20*, 1434−1441.
(30) Montes-Hernandez, G.; Renard, F. Time-resolved in situ Raman Spectroscopy of the Nucleation and Growth of Siderite, Magnesite and Calcite and their Precursors. *Cryst. Growth Des.* **2016**, *16*, 7218−7230.
(31) Urquidi, O.; Brazard, J.; LeMessurier, N.; Simine, L.; Adachi, T. B. M. In situ Optical Spectroscopy of Crystallization: One Crystal Nucleation at a Time. *Proc. Natl. Acad. Sci. U.S.A.* **2022**, *119*, No. e2122990119.
(32) Sosso, G. C.; Chen, J.; Cox, S. J.; Fitzner, M.; Pedevilla, P.; Zen, A.; Michaelides, A. Crystal Nucleation in Liquids: Open Questions and Future Challenges in Molecular Dynamics Simulations. *Chem. Rev.* **2016**, *116*, 7078−7116.
(33) Finney, A. R.; Salvalaglio, M. Molecular Simulation Approaches to Study Crystal Nucleation from Solutions: Theoretical Considerations and Computational Challenges. *Comput. Mol. Sci.* **2024**, *14*, No. e1697.
(34) Sun, W.; Booth, S.; Myerson, A.; Hughes, C.; Pan, H.; Coquerel, G.; Brandel, C.; Meekes, H.; Mazzotti, M.; Fabian, L.; Black, S.; Vekilov, P.; Back, K.; Toroz, D.; Lovelock, J.; Sefcik, J.; Rasmuson, A.; Breynaert, E.; Sear, R.; Hammond, R.; Ward, M.; Threlfall, T.; De Yoreo, J.; Davey, R.; Ristic, R.; Lewtas, K.; Roberts, K.; Hare, A.; Gich, M.; Cölfen, H.; Likhatskiy, M.; ter Horst, J.; Sommerdijk, N. Time and Space Resolved Methods: General Discussion. *Faraday Discuss.* **2015**, *179*, 247−267.
(35) Gebauer, D.; Wolf, S. E. Designing Solid Materials from Their Solute State: A Shift in Paradigms toward a Holistic Approach in Functional Materials Chemistry. *J. Am. Chem. Soc.* **2019**, *141*, 4490−4504.
(36) Jia, C.; Xiao, A.; Zhao, J.; Wang, P.; Fang, X.; Zhang, H.; Guan, B. A New Perspective on Crystal Nucleation: A Classical View on Non-Classical Nucleation. *Cryst. Growth Des.* **2024**, *24*, 601−612.
(37) Karthika, S.; Radhakrishnan, T. K.; Kalaichelvi, P. A Review of Classical and Nonclassical Nucleation Theories. *Cryst. Growth Des.* **2016**, *16*, 6663−6681.
(38) Kastrinakis, A.; Skliros, V.; Tsakiridis, P.; Perraki, M. CO_2 mineralised Nesquehonite: A New "Green" Building Material. *Mater. Proc.* **2021**, *5*, 60.
(39) Montes-Hernandez, G.; Renard, F.; Findling, N.; Auzende, A.-L. Formation of porous calcite mesocrystals from CO_2-H_2O-$Ca(OH)_2$ slurry in the presence of common domestic drinks. *CrystEngComm* **2015**, *17*, 5725−5733.
(40) Pimentel, C.; Montes-Hernandez, G.; Almarza-Cifuentes, P.; Kellermeier, M.; Van Driessche, A. E. S. From Waste to Value: Conversion of Calcium Sulfate to Vaterite via Carbon Capture and Storage. *Adv. Funct. Mater.* **2026**, *36*, No. e19977.

https://doi.org/10.1021/acs.cgd.6c00259
Cryst. Growth Des. XXXX, XXX, XXX−XXX